

# Modelling Combined Wave–Current Flows Using a RANS CFD Solver with Emphasis on the Effect of the Turbulent Closure Model

Maria João Teles, Michel Benoit and António A. Pires-Silva

**Abstract** The nearshore hydrodynamics and coastal circulation result from the contribution of a variety of phenomena which have complex physical interactions at different scales. Among these interactions, we focus here on the interaction between waves and current. In the present work, the evaluation and analysis of wave–current interactions is made through numerical simulations based on Reynolds averaged Navier–Stokes (RANS) equations, applied to the modelling of the complete flow motion, namely waves and current simultaneously (i.e., without decoupling the two phenomena). The advanced CFD code *Code\_Saturne* [1] is used for this purpose. The code is adapted for the study of waves and current interactions, using the arbitrary Lagrangian–Eulerian (ALE) method for dealing with free surface tracking, and considering turbulence effects in free surface flows. Several turbulence closure models are considered and compared, including two-equation models, namely  $k-\varepsilon$  and  $k-\omega$  models, largely used in this kind of studies for their simplicity, and also a second-order Reynolds stress transport model  $R_{ij}-\varepsilon$ . In particular, we show that imposing additional boundary conditions at the free surface was crucial to model the interaction effects. Numerical results are compared with experimental data from [2] for the following four types of flow conditions: (1) only current, (2) only waves, (3) waves following current and (4) waves opposing current. A detailed study of the changes in the vertical profiles of mean horizontal velocities and shear stresses when waves and current interact is

---

M. J. Teles (✉) · A. A. Pires-Silva  
Instituto Superior Técnico, TU Lisbon, Av. Rovisco Pais 1049-001 Lisbon,  
Portugal  
e-mail: mjteles@gmail.com

A. A. Pires-Silva  
e-mail: aps@civil.ist.utl.pt

M. Benoit  
Saint–Venant Laboratory for Hydraulics, Université Paris-Est (joint research unit between EDF R&D, CETMEF and Ecole des Ponts ParisTech), 6 quai Watier, BP 49 78401 Chatou, France  
e-mail: michel.benoit@saint-venant-lab.fr

presented, with a discussion about the effects of the turbulence closure model used in the simulations.

**Keywords** Wave–current interaction • Turbulence model • *Code\_Saturne* • Eddy viscosity • Reynolds shear stress

## 1 Introduction

The interaction between waves and current in free surface flows is of a great importance for the hydrodynamics of coastal waters. It has been a subject of several experimental and numerical studies. The most important issues in such wave–current combined environments (in comparison with the cases where either only waves or only current is present) are the changes in the horizontal and vertical mean velocities and in the Reynolds shear stresses.

The design of coastal protections and harbour sheltering structures, the evaluation of sediment transport and coastal erosion, the assessment of wave power available at a certain spot or the impact of a farm of wave energy converters are examples of possible applications that will benefit from an enhanced knowledge and modelling of the effects of this two-way wave–current interaction.

The present work aims at studying the changes that occur when waves are superimposed on a turbulent current, with particular attention to the modifications of the vertical profiles of (1) the mean horizontal velocity, (2) shear stresses and (3) turbulent (eddy) viscosity. For this purpose, a RANS CFD model capable of resolving all this combined effects will be employed, namely *Code\_Saturne* [1]. Some sensitivity tests will also be made regarding the turbulence closure model that exhibit the best performance to model this kind of flows.

## 2 Laboratory Data

A series of laboratory experiments were carried out by Umeyama [2] in a wave–current flume. This flume was 25 m long, 0.7 m wide. The bottom of the flume was flat, and it was filled with a water depth of 0.20 m. The flume was equipped with a flow circulation circuit able to deliver a constant discharge, which was about  $Q = 59$  l/s for all the tests considered below (when a current is present).

Regular (monochromatic) waves were generated through a piston-type wave maker located at an end of the flume, and dissipated with a wave absorber at the other end of the flume. A series of four pairs of wave parameters (height and period) were successively considered (see Table 1).

Tests were run under the four following conditions: (1) current without waves (or “only current”), (2) waves without current (or “only waves”), (3) waves

**Table 1** Wave heights and wave periods for the four different test cases from [2]

Tests	T1	T2	T3	T4
Wave height (m)	0.0202	0.0250	0.0260	0.0280
Wave period (s)	0.9	1.0	1.2	1.4

following current, and (4) waves opposing current. For each test, vertical profiles of mean velocities and shear stresses were measured at a distance of 10.5 m from the wave generator, by a laser Doppler anemometer.

### 3 Code\_Saturne Model

#### 3.1 Introduction

*Code\_Saturne* [1] is a CFD code for laminar and turbulent flows in two- and three-dimensional domains, developed at the R&D division of Electricité de France (EDF). It solves the Reynolds averaged Navier–Stokes (RANS) equations by using a finite volume method. The equations are written in a conservative form and then integrated over the control volumes of each cell of the 3D mesh:

$$\frac{\partial \rho}{\partial t} + \nabla \cdot (\rho \underline{u}) = \Gamma \tag{1}$$

$$\rho \frac{\partial \underline{u}}{\partial t} + \nabla \cdot (\rho \underline{u} \otimes \underline{u}) = -\nabla(P) + \nabla \cdot (\underline{\underline{\tau}} - \rho \underline{\underline{R}}) + \underline{S}_u \tag{2}$$

where  $\rho$  is the fluid density,  $\underline{u}$  the fluid velocity vector,  $\Gamma$  a mass source term,  $P$  the pressure,  $\underline{\underline{\tau}}$  the viscous stress tensor,  $\underline{\underline{R}}$  the Reynolds stress tensor and  $\underline{S}_u$  a momentum source term.

In order to close the system (1)–(2), a model has to be introduced for the turbulent correlations of the Reynolds stress tensor  $\underline{\underline{R}}$ . *Code\_Saturne* has implemented a large range of first- and second-order turbulence models (see Ref. [1] for details). In the present work, it was decided to proceed to the analysis of the wave–current interactions with the two-equation models  $k-\epsilon$  [3] and  $k-\omega$  [4] and a Reynolds stress model (RSM), the so-called  $R_{ij}-\epsilon$  SSG model [5].

The first two models were chosen due to their relative simplicity and because they are often used in this kind of studies of wave–current interaction. The second-order turbulence closure model choice was made since the  $R_{ij}-\epsilon$  model accounts for the directional effects of the Reynolds stress fields (anisotropy) and does not rely on the eddy viscosity hypothesis. It solves six transport equations for the six components of the Reynolds stress tensor and one equation for the turbulent dissipation rate  $\epsilon$ , without making any a priori assumption on the eddy viscosity distribution  $\nu_t$  (which can nevertheless be estimated a posteriori from the results of that model).

Regarding the modelling of a time-varying free surface, *Code\_Saturne* has incorporated in its code the arbitrary Lagrangian–Eulerian (ALE) method. With this module, the Navier–Stokes equations gain a new term, which is the velocity of the mesh. For each time step, the mesh is updated accordingly. In this way, it is possible to represent of the free surface variations due to waves.

### 3.2 Model Set-Up

Regarding the model set-up, some conditions have to be ensured. For the mesh generation, in the direction of wave propagation, a number of about 10 cells per wave length had to be guaranteed in order to reach a good representation of the surface waves. On the other hand, right next to the moving wall corresponding to the wave maker, the mesh velocity had to be compatible with the fluid velocity in order to avoid mesh crossover and provoke the divergence of the simulation.

As *High Reynolds* number models were used, the mesh near the bottom could not be too refined. At the same time, a sufficiently fine resolution was required in the same region in order to analyse some important effects, such as the roughness influence on the vertical profile of the measured quantities. On Fig. 1 the computational domain representative of experiments from [2] is shown.

Waves propagate in the positive  $x$  direction. In order to generate waves, *Code\_Saturne* was forced with a horizontal motion of the mesh on the left lateral boundary. To minimize undesirable super-harmonic free waves, a second-order wave board displacement of the piston-type wave maker was applied on the flume. The following expression [6] for the wave board motion  $X_0(t)$  (3) was introduced:

$$X_0(t) = \frac{H}{2m_1} \sin(\sigma t) + \frac{H^2}{32h} \left( \frac{3 \cosh(kh)}{\sinh^3(kh)} - \frac{2}{m_1} \right) \sin(2\sigma t) \tag{3}$$

$$m_1 = \frac{4 \sin h(kh)}{\sin h(2kh) + 2kh} \left[ \sin h(kh) + \frac{(1 - \cos h(kh))}{kh} \right] \tag{4}$$

where  $k$  represents here the wave number (not to be confused with the turbulent kinetic energy, also denoted  $k$ ),  $h$  the water depth,  $H$  the wave height,  $\sigma$  the relative angular wave frequency and  $t$  the time. The signal given by Eq. (3) had to be

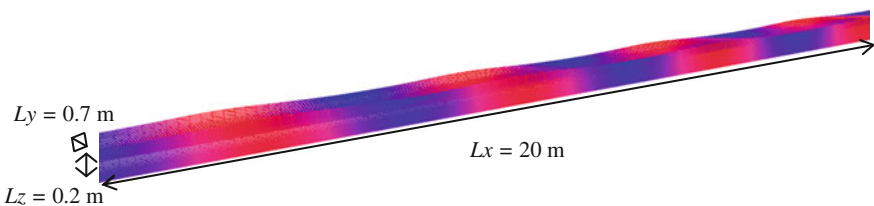


**Fig. 1** Computational domain representative of experiments from [2]

progressively imposed at the lateral boundary, to avoid a sudden horizontal movement of the mesh and thus mesh crossover.

The reflections of waves at the right end of the channel were dealt with an artificial beach imposed at the downstream boundary, based on a viscous damping term that increased linearly from the bottom to the free surface.

Regarding the boundary conditions, special attention was devoted to the free surface. An additional condition had to be imposed for the turbulent dissipation  $\varepsilon$  [7] in order to get accurate results near the free surface.

$$\varepsilon = \frac{k^{3/2}}{\alpha h} \quad (5)$$

where is  $k$  the turbulent kinetic energy at the water surface and  $\alpha = 0.18$  an empirical constant. With the imposition of this condition, the turbulent dissipation  $\varepsilon$  increases and the eddy viscosity decreases towards the free surface. These variations were observed during the experiments made by [3].

## 4 Discussion of Results

### 4.1 Effects of the Turbulence Closure Model on the Mean Horizontal Velocity

As mentioned in Sect. 2, the experiments from [2] were performed with different wave heights and periods. These conditions for the four test cases were simulated with *Code\_Saturne* [8]. In the following, comparisons between numerical results and data of the vertical profile of the mean horizontal velocity for the test T1 (see Table 1) are shown for “only current” and “only waves” (Fig. 2), “waves following current” and “waves opposing current” (Fig. 3). A sensitivity analysis was made regarding the turbulence closure model that best describes this test case. It must be highlighted that this sensitivity test is made without any parameterization besides the default conditions and settings defined in *Code\_Saturne*, with the exception of the boundary condition (Eq. 5) that was imposed for each test.

As it can be observed on these figures, the three turbulence closure models can represent quite well the vertical profile of mean horizontal velocity for the case “only current”. Nevertheless, for the “only waves” case, the  $R_{ij-\varepsilon}$  model is the one that best fits the experimental data over the water column.

When waves are superimposed on a turbulent current, the profile of mean horizontal velocity is changed (Fig. 3). While the mean horizontal velocities near the free surface are reduced for the “waves following current” case, these velocities are increased when waves are opposing the current. This was observed by [2] and *Code\_Saturne* was able to well reproduce this change in the current profile with the  $R_{ij-\varepsilon}$  model, especially when waves are following the current. When waves are opposing the current, even if the velocities are a bit

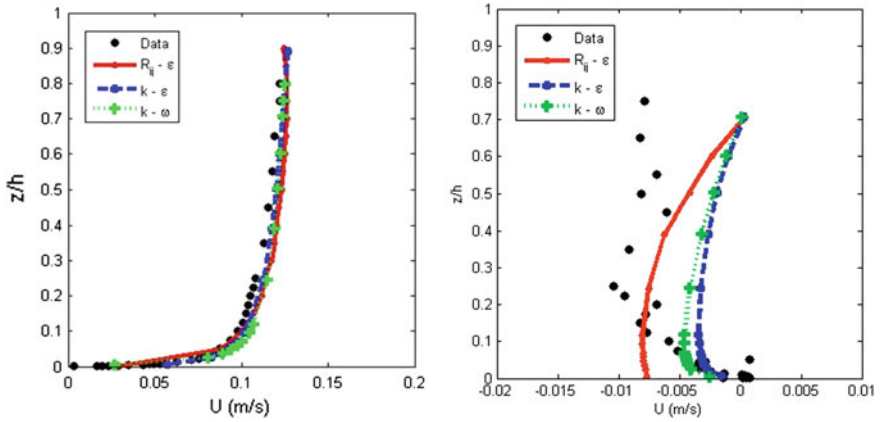


**Fig. 2** Mean horizontal velocity vertical profile for “only current” (*on the left*) and “only waves” (*on the right*). Comparison with data from [2]

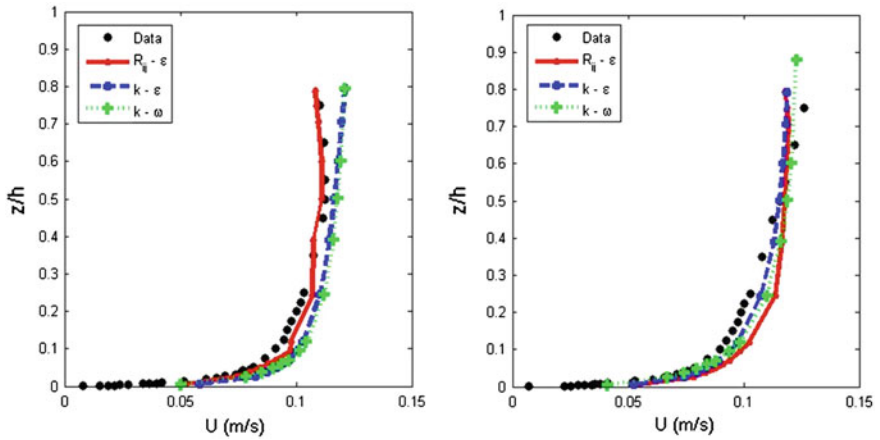


**Fig. 3** Mean horizontal velocity vertical profile for “waves following current” (*on the left*) and “waves opposing current” (*on the right*). Comparison with data from [2]

underestimated near the free surface and a bit overestimated in the middle of the water column, a good overall agreement is observed.

### 4.2 Effects of the Turbulence Closure Model on the Reynolds Shear Stress

We also conducted a sensitivity analysis regarding the changes in the vertical profile of the Reynolds shear stress  $R_{xz} = -\overline{u'w'}$  when waves and current interact

with the aim to determine which turbulence closure model was the most appropriate to describe these changes. In the following, we show the comparison between *Code\_Saturne* results and experimental data for “only current” on Fig. 4, “only waves” on Fig. 5 and “waves following current” and “waves opposing current” on Fig. 6.

As it can be seen from Fig. 4, all the three closure turbulence models are capable to correctly reproduce the shear stress profile obtained through experimental data when there is only a current in the channel. For what concerns the “only waves” test case, the shear stress profile is almost zero, as it can be observed on experimental data. In this case, *Code\_Saturne* model overestimates the shear stress values over the whole water column when the  $k-\epsilon$  and  $k-\omega$  are applied (Fig. 5 on the left). On the right side of Fig. 5, it can be seen that a good agreement is found between the results from  $R_{ij}-\epsilon$  model and data.

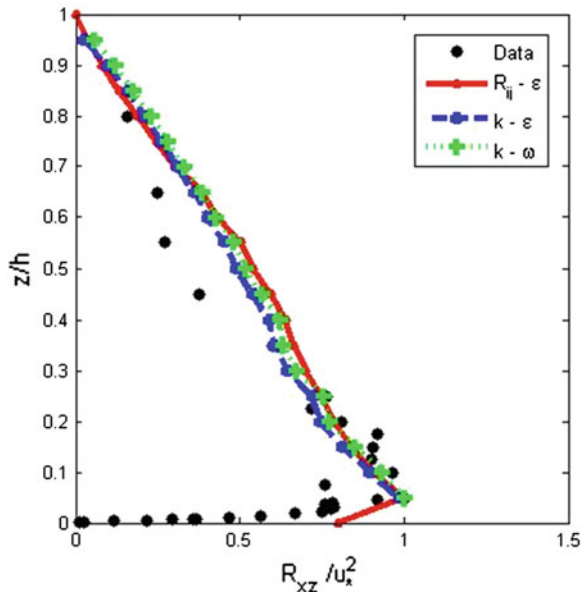
When waves are superimposed on the current, the dimensionless Reynolds shear stress profile is in general well simulated throughout the water depth with the three turbulence closure models.

From the tests made with *Code\_Saturne*, it can thus be confirmed that the model is capable to reproduce quite well the wave–current interaction effects.

### 4.3 Analysis of the Vertical Profile of the Eddy Viscosity

Some experiments were made by [9] in a flume with only a current, and measures of the vertical profile of the eddy viscosity were obtained. Comparing this data

**Fig. 4** Vertical profile of the dimensionless Reynolds shear stress  $\frac{R_{xz}}{u_*^2} = \frac{-\overline{u'w'}}{u_*^2}$  for “only current” (i.e., no waves). Comparison with data from [2]



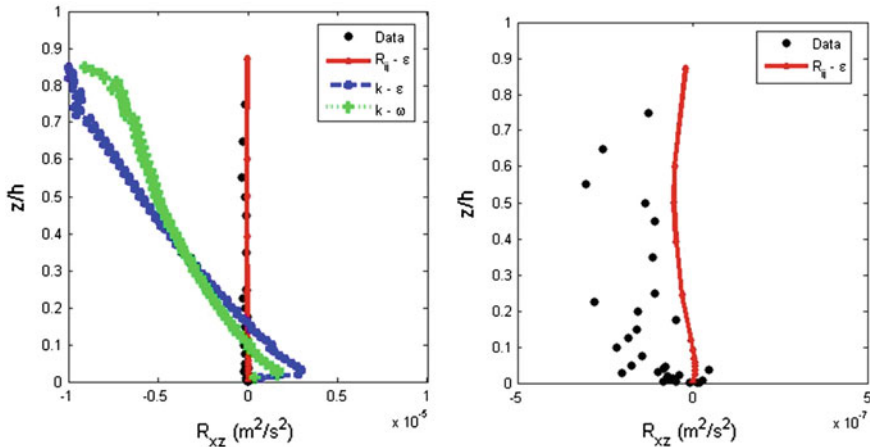


**Fig. 5** Vertical profile of the Reynolds shear stress  $R_{xz} = -\overline{u'w'}$  for “only waves” (i.e., no current) with the three turbulence closure models (*on the left*) and with only  $R_{ij}-\epsilon$  model (*on the right*)

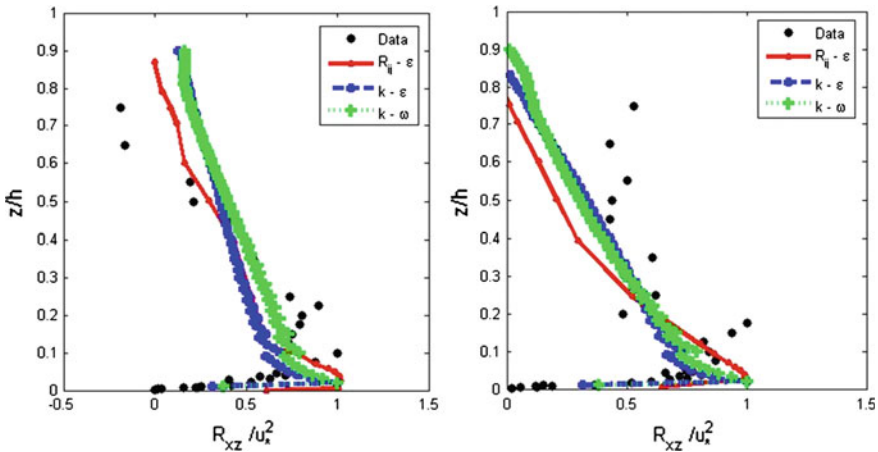
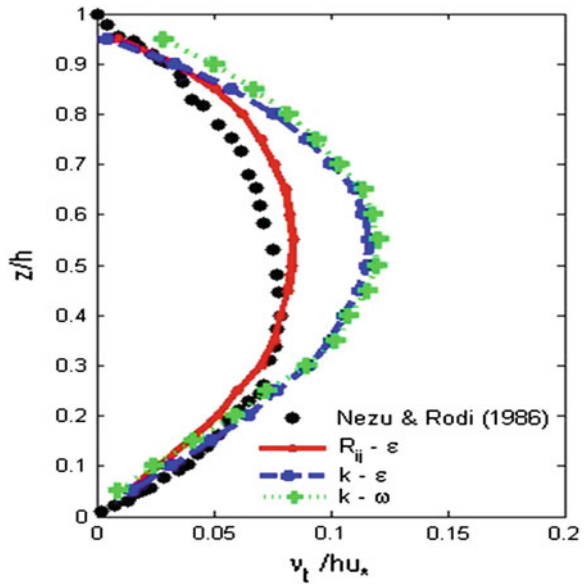


**Fig. 6** Vertical profile of the dimensionless Reynolds shear stress  $\frac{R_{xz}}{u_*^2} = \frac{-\overline{u'w'}}{u_*^2}$  for “waves following current” (*on the left*) and “waves opposing current” (*on the right*). Comparison with data from [2]

with *Code\_Saturne* results obtained with the application of the three turbulence closure models, it can be seen that the same order of dimensionless values was achieved from all the models even if the  $k-\epsilon$  and  $k-\omega$  slightly overestimate it (Fig. 7). It should be noticed that the behaviour obtained in the turbulent viscosity profile (with a parabolic shape over depth) is achieved due to the boundary condition imposed for the turbulent dissipation rate the free surface [see Eq. (5)].



**Fig. 7** Vertical profile of the non-dimensional eddy viscosity  $v_t/(hu_s)$  for “only current”. Comparison with data from [9]



On Fig. 8, the turbulent viscosity profiles for “waves following current” (on the left side) and “waves opposing current” (on the right side) are also shown.

In order to get a simple parameterization of the eddy viscosity development over the water column in this study, where waves and current interact, a dimensionless relation between the turbulent viscosity ( $v_t$ ), acceleration due to gravity ( $g$ ), mass transport velocity ( $U$ ), water depth ( $h$ ), wave period ( $T$ ), wave length ( $L$ ) and wave height ( $H$ ) was sought. After considering several possible

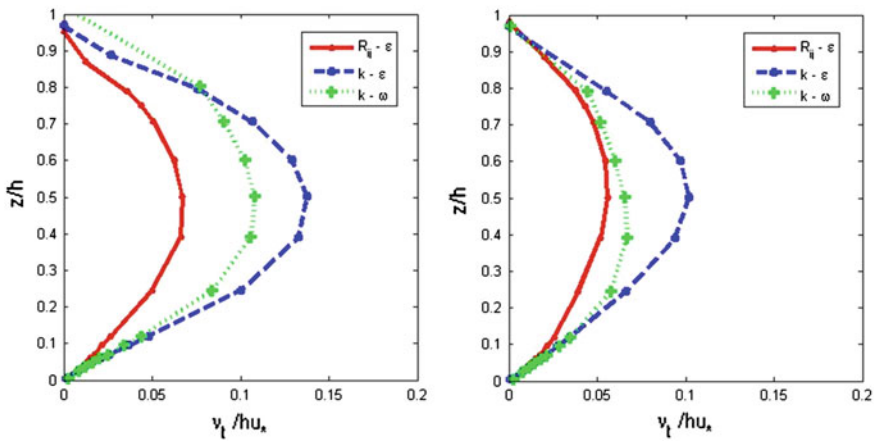


**Fig. 8** Vertical profile of the non-dimensional eddy viscosity for “waves following the current” (on the left) and “waves opposing the current” (on the right)

dependences, it was found that the non-dimensional eddy viscosity  $\nu_t/(gUT^2)$  at each relative elevation from the bottom ( $z/h$ ) seems to decrease approximately linearly with the Ursell number ( $HL^2/h^3$ ), as illustrated in Fig. 9, where the various variables correspond to the results of the simulations made with *Code\_Saturne* with the application of the Reynolds stress transport model  $R_{ij}-\epsilon$ .

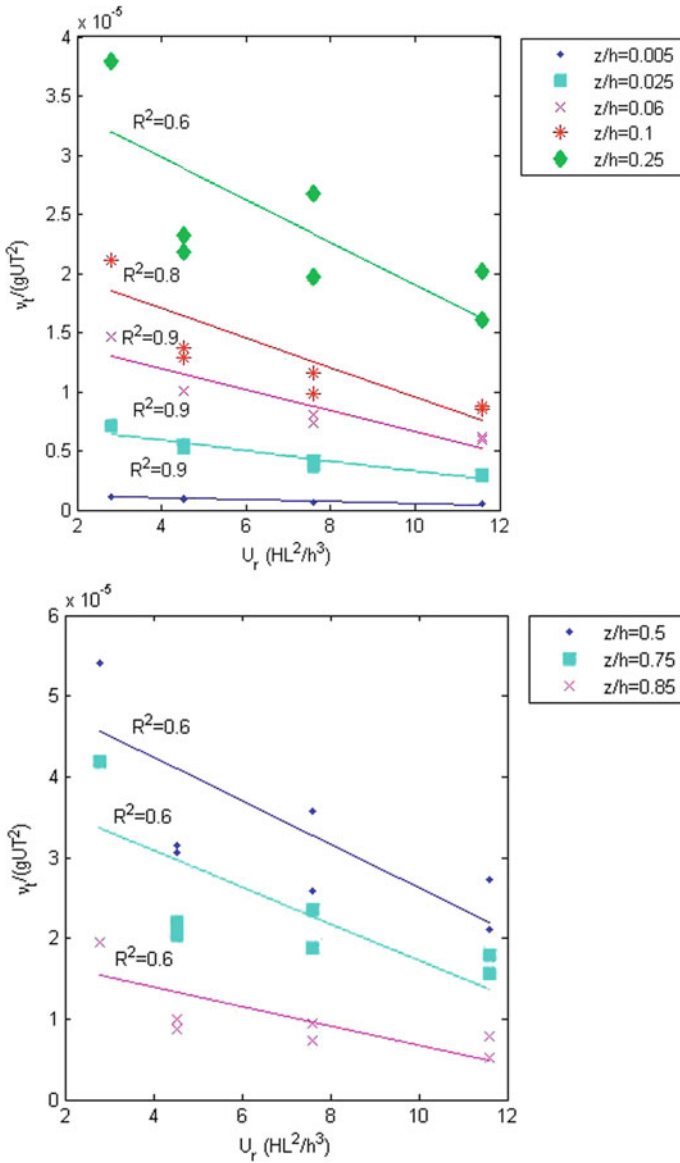


**Fig. 9** Variations of the non-dimensional eddy viscosity  $\nu_t/(gUT^2)$  for each  $z/h$  level as a function of the Ursell number  $HL^2/h^3$

This tentative parameterization of the eddy viscosity needs, however, to be validated against a more extensive set of data. If confirmed, it could be used for instance in more simplified simulation models that rely on the eddy viscosity assumption for the turbulence closure scheme.

### 4.4 Analysis of the Vertical Profile of the Dimensionless Kinetic Turbulent Energy and Turbulent Dissipation

The dimensionless turbulent kinetic energy and the dimensionless dissipation rate are shown below with the three turbulence closure models for the cases “only current” (Fig. 10), “waves following current” (Fig. 11) and “waves opposing current” (Fig. 12). Semi-empirical formulas [10] were also included for the “only current” case and used to estimate the dimensionless turbulent kinetic energy (6) and dissipation rate (7).

$$\frac{k}{u_*^2} = 4.78 e^{(-2z/h)} \tag{6}$$

$$\frac{\epsilon h}{u_*^3} = 9.8 \left(\frac{z}{h}\right)^{-1/2} e^{(-3z/h)} \tag{7}$$

For the “only current” case, it can be observed that the profiles of the non-dimensional turbulent intensities are quite similar to each other. The comparison of the numerical simulations with the semi-empirical curves shows, in general, the same order of magnitude.

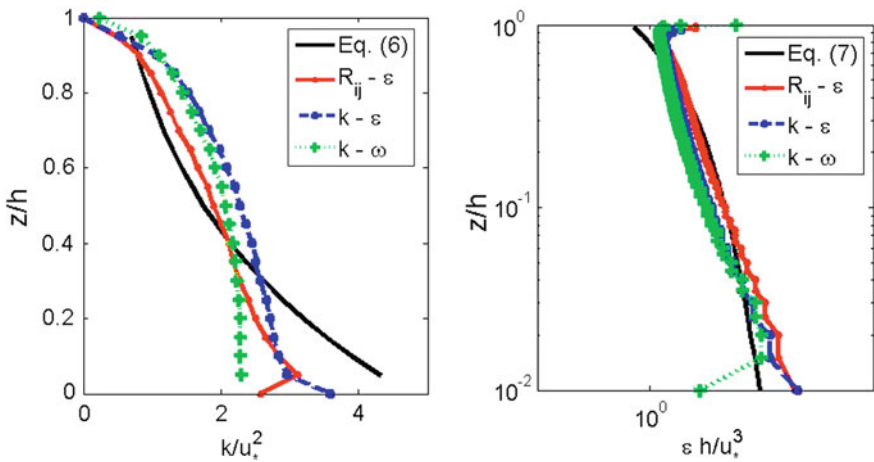


**Fig. 10** Vertical profiles of the dimensionless kinetic turbulent energy and turbulent dissipation for “only current” (i.e., no waves)

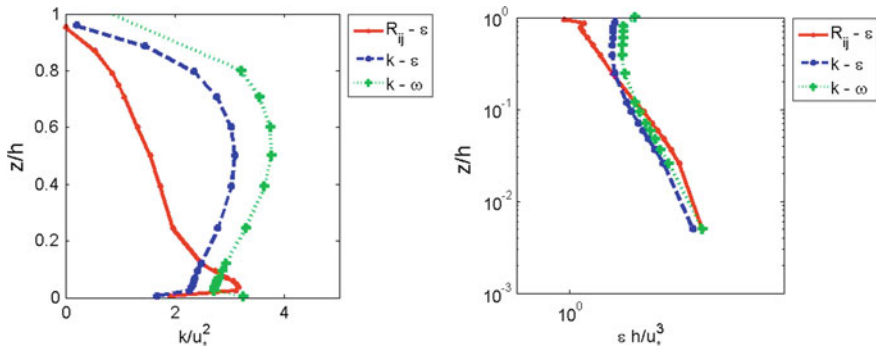


**Fig. 11** Vertical profiles of the dimensionless kinetic turbulent energy (*on the left*) and turbulent dissipation (*on the right*) for “waves following the current”

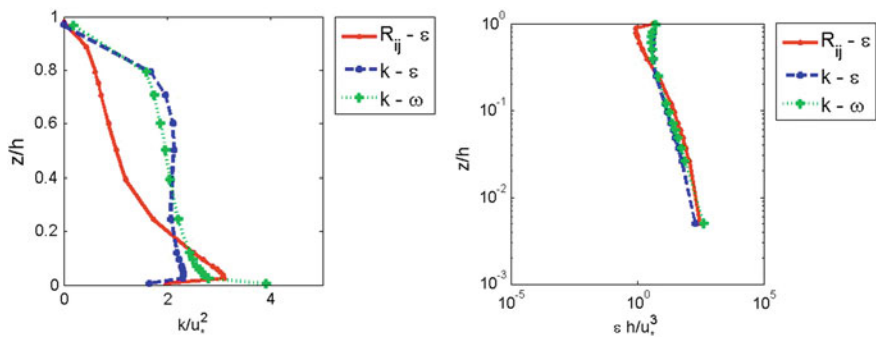


**Fig. 12** Vertical profiles of the dimensionless kinetic turbulent energy (*on the left*) and turbulent dissipation (*on the right*) for “waves opposing the current”

Moreover, it was decided to also get the dimensionless turbulent energy and turbulent dissipation for “waves following the current” and “waves opposing the current” cases even if no empirical formulas were used.

### 5 Conclusions

*Code\_Saturne* model was tested in free surface flows in a combined wave–current environment. Data from [2] was used to verify the performances and capabilities of the model. Different tests were available: “only current”, “only waves”, “waves following current” and “waves opposing current”. A sensitivity test was also made, regarding the turbulence closure model that could best represent this kind of combined flows. Three turbulence closure models were used, namely two two-equation models,  $k-\epsilon$  and  $k-\omega$  and a RMS,  $R_{ij}-\epsilon$ .

The vertical profile of the mean horizontal velocity is changed when waves are superimposed on a current. *Code\_Saturne* was able to well reproduce the reduction of mean velocities near the free surface when waves are following the current and the increase of velocity when waves are opposing the current. Not only is the mean horizontal velocity profile changed, but also the Reynolds shear stress profile. When waves and current interact the bed shear stress decreases when comparing with the only current case. Once again, *Code\_Saturne* gave quite good reproduction of this trend throughout the depth.

Regarding the sensitivity tests for the different turbulence closure model, the second-order RMS,  $R_{ij}-\varepsilon$ , has showed, in this case, to have the best performance to model this kind of flows. This second-order turbulence model is more general (and thus in principle more accurate and powerful) than the two-equation models. Indeed, it accounts for the directional effects of the Reynolds stress fields (anisotropy) and does not include the eddy viscosity modelling hypothesis in contrary to the two-equation models.

Finally, the expression (5) for the turbulent dissipation at the free surface, as proposed by Celik and Rodi [7], has shown to be essential to correctly reproduce the vertical profiles of Reynolds stress and eddy viscosity.

**Acknowledgments** Maria João Teles would like to acknowledge the support of a Ph.D. grant (SFRH/BD/61269/2009) from FCT (Fundação para a Ciência e Tecnologia), Portugal.

## References

1. Archambeau, F., Méchitoua, N., & Sakiz, M. (2004). *Code\_Saturne*: A finite volume method for the computation of turbulent incompressible flows—industrial applications. *International Journal of Finite Volumes*, 1(1), 1–62.
2. Umeyama, M. (2005). Reynolds stresses and velocity distributions in a wave–current coexisting environment. *Journal of Waterway, Port, Coastal and Ocean Engineering*, 131(5), 203–212.
3. Guimet, V., & Laurence, D. (2002). A linearised turbulent production in the  $k - \varepsilon$  model for engineering applications. In W. Rodi & N. Fueyo (Eds.), *5th Engineering Turbulence modelling and Measurements*. Elsevier.
4. Menter, F. R. (1993). *Zonal two equation  $k-\omega$  turbulence models for aerodynamic flows*. AIAA Paper 93-2906.
5. Speziale, C. G., Sarkar, S., & Gatski, T. B. (1991). Modeling the pressure-strain correlation of turbulence: An invariant dynamical systems approach. *Journal of Fluid Mechanics*, 227, 245–272.
6. Dean, R. G., & Dalrymple, R. A. (1991). *Water wave mechanics for engineers and scientists*. Singapore: World Scientific Press.
7. Celik, I., & Rodi, W. (1984). Simulation of free surface effects in turbulent channel flows. *Physicochemical Hydrodynamics*, 5, 217–227.
8. Teles, M. J., Pires-Silva, A. A., Benoit, M. (2013). Numerical modelling of waves and current interactions at a local scale. *Ocean Modelling*, 68, 72–87.
9. Nezu, I., & Rodi, W. (1986). Open channel flow measurements with a laser Doppler anemometer. *Journal of Hydraulic Engineering*, 112(5), 335–355.
10. Nezu, I., & Nakagawa, H. (1993). *Turbulence in open-channel flows*. Rotterdam: AA Balkema.